Preparation of an Organomontmorillonite Master Batch and Its Application to High-Temperature-Vulcanized Silicone-Rubber Systems

Jincheng Wang, Yuehui Chen

College of Chemistry and Chemical Engineering, Shanghai University of Engineering Science, Shanghai 201620, China

Received 26 May 2007; accepted 22 July 2007
DOI 10.1002/app.27134
Published online 29 October 2007 in Wiley InterScience (www.interscience.wiley.com).

ABSTRACT: *N,N*-Di(2-hydroxyethyl)-*N*-dodecyl-*N*-methyl ammonium chloride was used as an intercalation agent to treat Na^+-montmorillonite and form a novel type of organic montmorillonite (OMMT). An OMMT master batch (OMMT-MB) was prepared by solution intercalation and was used in the preparation of high-temperature-vulcanized silicone rubber (HTV-SR)/OMMT-MB nanocomposites. The properties, such as the tensile and thermal stability, were researched and compared with those of composites directly incorporated with OMMT or aerosilica. A combination of Fourier transform infrared spectroscopy, wide-angle X-ray diffraction, and transmission electron microscopy studies showed that HTV-SR/OMMT-MB composites were on the nanometer scale, and their structure was somewhat hindered by the presence of OMMT. The results showed that the tensile properties of HTV-SR/OMMT-MB and HTV-SR/OMMT systems were better than those of pure HTV-SR. Compared with those of HTV-SR/OMMT-20%, the tensile strength and elongation at break of HTV-SR/OMMT-MB-20% were improved about 1.5 and 0.9 times, respectively. This was probably due to the nanoeffect of the exfoliated silicate layers. Moreover, the tensile strength of HTV-SR/OMMT-MB-20% was nearly equal to that of HTV-SR/aerosilica-20%, and the elongation at break even showed much improvement. Additionally, the thermal degradation center temperature of the HTV-SR/OMMT-MB-20% nanocomposite was increased by 30°C compared with that of the HTV-SR/OMMT-20% composite. © 2007 Wiley Periodicals, Inc. J Appl Polym Sci 107: 2059–2066, 2008

Key words: nanotechnology; organoclay; rubber

INTRODUCTION

In the past 20 years, much attention has been focused on polymer-layered silicate nanocomposites with polymer-chain intercalating galleries of adjacent silicate layers.[1–11] These polymers usually form exfoliated or intercalated nanocomposites that have improved or new properties in comparison with the bulk polymer.

The reinforcement of rubbers is expressed by an enhancement of the tensile strength, thermal stability, modulus, and abrasion resistance of the vulcanizates. The main aim of filler addition is to improve certain properties and cheapen the compound.[12] Among several fillers, aerosilica is the most important reinforcing agent used in the silicone-rubber (SR) industry. Because of its high price, easy conglomeration, and harmfulness to workers' health, researchers have focused on the development of other reinforcing fillers such as montmorillonite (MMT) to replace aerosilica. Wang et al.[13] investigated the mechanical properties and thermal stability of SR/organic montmorillonite (OMMT) hybrids synthesized by means of solution intercalation. The results showed that the physical and mechanical properties of an SR system with 1 phr OMMT were nearly equal to those of SR with 3 phr aerosilica because of the exfoliation of OMMT and the resultant nanoeffect in the system. Zhou et al.[14] synthesized a novel exfoliated SR/clay nanocomposite with hydroxyl-terminated polydimethylsiloxane and organic clay. The mechanical properties of the nanocomposites prepared by different intercalation agents were compared, and the reinforcing and intercalation mechanisms were discussed. Zheng et al.[15] reported the polymerization of SR/MMT composites with octamethyl cyclotetrasiloxane and MMT as raw materials via monomer intercalation and ring-opening polymerization. The results indicated that MMT had an inhibition effect on the anionic ring-opening polymerization and was an ideal initiator in cationic polymerization.

Typically, MMT, a layered clay mineral, is a hydrated alumina silicate clay. It is composed of

Correspondence to: J. Wang (wjc406@263.net).

Contract grant sponsor: Shanghai Educational Commission Common Project; contract grant numbers: 06NZ006 and 06NZ008.

Contract grant sponsor: Shanghai Leading Academic Discipline Project; contract grant number: p1402.

Journal of Applied Polymer Science, Vol. 107, 2059–2066 (2008)

units of two silicate tetrahedral sheets with a certain alumina octahedral sheet. The silicate layers of MMT are planar, stiff, and about 10 Å in thickness and 1000–2000 Å in length and width. They do not occur as isolated individual units but aggregate to form crystalline structures.[16] For the efficient improvement of the properties of polymer/MMT composites, the basal spacing of MMT should be made accessible to the polymer chains. This may be realized through cation exchange between MMT and organic ammonium salts, which yields OMMT. However, the efficiency of OMMT in improving the properties of polymer materials depends not only on the surface nature of the OMMT but also on the state of the polymeric materials. High-temperature-vulcanized silicone rubber (HTV-SR) is a kind of solid-state material. It is usually operated at room temperature in a plasticator during production. This is not beneficial for its molecular chain to insert into the silicate layers and for the silicate layers to disperse in the polymeric matrix to a nanometer degree.

To overcome these problems, solution intercalation and OMMT master batch (OMMT-MB) techniques were used in the preparation of HTV-SR composites. Properties such as the tensile strength and thermal stability were researched and compared. Then, a combination of Fourier transform infrared (FTIR) spectroscopy, wide-angle X-ray diffraction (WAXD), and transmission electron microscopy (TEM) studies showed that HTV-SR/OMMT-MB composites were on the nanometer scale. The results demonstrated that the use of solution intercalation and OMMT-MB techniques could greatly improve the physical and mechanical properties of HTV-SR because of a nanoeffect of the silicate layers in the system.

EXPERIMENTAL

Materials

Industrial-grade Na^+-montmorillonite (Na^+-MMT) was obtained from Zhejiang Fenghong Clay Co. (Zhejiang, China). Chemically pure *N,N*-di(2-hydroxyethyl)-*N*-dodecyl-*N*-methyl ammonium chloride was received from Zhejiang Chemical Agent Co. (Zhejiang, China). Industrial-grade aerosilica was bought from Shanghai Huitian New Materials Co. (Shanghai, China). HTV-SR (the two components were gum and 2,4-terbutyl hexane peroxide) was supplied by Shanghai Huitian New Materials Co. (Shanghai, China).

Preparation of OMMT

A 500-mL, round-bottom, three-necked flask with a mechanical stirrer, thermometer, and condenser with a drying tube was used as a reactor. *N,N*-Di(2-hydroxyethyl)-*N*-dodecyl-*N*-methyl ammonium chloride (3.52 g) was dissolved in 120 mL of an ethanol and water mixture (1 : 1 w/w). MMT (10 g) was gradually added to this solution. The resultant suspension was vigorously stirred for 2 h. The treated MMT was repeatedly washed with deionized water. The filtrate was titrated with 0.1*N* $AgNO_3$ until no precipitate of AgCl was formed. This ensured the complete removal of chloride ions. The filter cake was then placed in a vacuum oven at 80°C for 12 h for drying. The dried cake was ground to obtain the OMMTs.

Preparation of OMMT-MB

Gum (70, 60, or 50 g) was dissolved in a 100-mL toluene solution. It was stirred for 2 h, after which a homogeneous solution was obtained. OMMT (30, 40, or 50 g) was gradually added to this solution. The resultant mixture was vigorously stirred for 2 h. The treated system was then placed in a vacuum oven at 80°C for 12 h to ensure the complete removal of the toluene solvent. Finally, OMMT-MB-30%, OMMT-MB-40%, or OMMT-MB-50% was obtained.

Preparation of the HTV-SR composites

OMMT (15, 20, or 25 g) was added to 85, 80, or 75 g of an HTV-SR system, 50 g of 30, 40, or 50 wt % OMMT-MB was added to 50 g of an HTV-SR system, or 20 g of aerosilica was added to 80 g of an HTV-SR system on a double-roller plasticator. After 20 min of mixing, 0.8 g of 2,4-terbutyl hexane peroxide was added, and different types of composites were prepared. The sheeted compounds were then conditioned at 20°C for 24 h before curing. These composites were then cured at 175°C for 5 min under 15 MPa of pressure on an electrically heated press, after which elastic films were obtained. These films were denoted HTV-SR/OMMT-15%, HTV-SR/OMMT-20%, HTV-SR/OMMT-25%, HTV-SR/OMMT-MB-15%, HTV-SR/OMMT-MB-20%, HTV-SR/OMMT-MB-25%, and HTV-SR/aerosilica-20%, respectively.

Characterization

The tensile tests were carried out with an Instron model 4204 instrument (New York) at room temperature with a crosshead speed of 500 mm/min. The HTV-SR composites were manufactured in a standard dumbbell shape. All measurements were repeated five times, and medium data were obtained. Thermogravimetric analysis (TGA) of the samples was carried out at 10°C/min under air (flow rate 5×10^{-7} m^3/s, air liquid grade) with a Universal V3.8B TA microbalance. In each case, the mass of the samples used was fixed at 10 mg, and then they

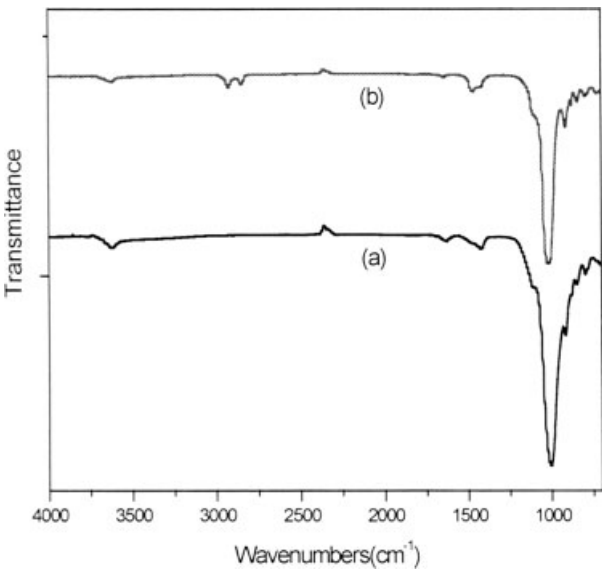

Figure 1 FTIR spectra of (a) MMT and (b) OMMT.

were positioned in open vitreous silica pans. The precision of the temperature measurements was 1°C over the whole range of temperatures.

To measure the change of the gallery distance of MMT, OMMT, and HTV-SR composites before and after intercalation, WAXD was performed at room temperature with a Rigaku D-Max/400 (Tokyo, Japan) X-ray diffractometer. The X-ray beam was nickel-filtered Cu Kα (λ = 0.154 nm) radiation operated at 50 kV and 150 mA. X-ray diffraction data were obtained from 1 to 10° (2θ) at a rate of 2°/min. Infrared transmission spectra of MMT, OMMT, and HTV-SR composites were obtained with a model Dos X FTIR spectrometer from Nicolet Corp. (New York). The scan range was from 4000 to 400 cm^{-1} with a resolution of 2 cm^{-1}. The samples for TEM were first prepared by the microtoming of the composites into 80–100-nm-thick slices at −90°C. The graphs were obtained with an H-800 instrument (Tokyo, Japan) at an acceleration voltage of 200 kV.

RESULTS AND DISCUSSION

Analysis of OMMT

The FTIR spectra of the original MMT and OMMT are shown in Figure 1. The 3620–3650-cm^{-1} peak was caused by the stretching of —OH. This was due to the physical and chemical water in Na^+-MMT. The peaks at 1030 and 700 cm^{-1} resulted from the stretching vibrations of Si—O and Al—O bonds in the MMT structure. In the spectra of OMMT, except for the peaks in MMT, the presence of new peaks at 2800–3000 and 1469 cm^{-1} was indicated. These were caused by C—H stretching and bending absorptions in the organic intercalation agent. The disappearing peaks at 1640 cm^{-1} (belonging to bending vibrations of O—H) illustrated the disappearance of inorganic water that existed in the silicate layers in MMT. This environment was beneficial for exchanging Na^+ cations in MMT and $-\overset{|}{\underset{|}{\overset{+}{N}}}-$ cations in the intercalation agents.[17–19]

The WAXD patterns of the original MMT and OMMT are shown in Figure 2. Figure 2(a) [WAXD of pure MMT] shows a characteristic peak at 2θ = 6°, which was assigned to the 001 basal reflection. In Figure 2(b), there are three peaks in the WAXD spectrum. This indicates the different expansion degrees of silicate layers in OMMT, which were probably due to the following reasons. First, the structure of the new intercalation agent could have had some influence on the enlargement of silicate-layer basal spacing in OMMT. The strong polarity of —OH groups, branching chains of dihydroxyethyl, and space distributing morphology of molecular chains of this intercalation agent may have influenced the Coulomb force between the silicate layers and made the space between the silicate layers of OMMT not uniform. Second, the structure and properties of the inorganic MMT, which was produced by Zhejiang Fenghong Clay, may have been different from those of other common MMTs. The Coulomb force between the silicate layers of this MMT may not have been uniform.[20] The data for MMT and OMMT, calculated by the Bragg formula ($2d \sin\theta = n\lambda$), are summarized in Table I.

MMT clay is a phyllosilicate mineral. Cations such as Na^+, K^+, and Ca^{2+}, compensate the negative charge that exists in the crystal lattice of each silicate layer in MMT. Polar molecules such as *N*,*N*-di(2-hydroxyethyl)-*N*-dodecyl-*N*-methyl ammonium chloride, which can make MMT more organophilic, can

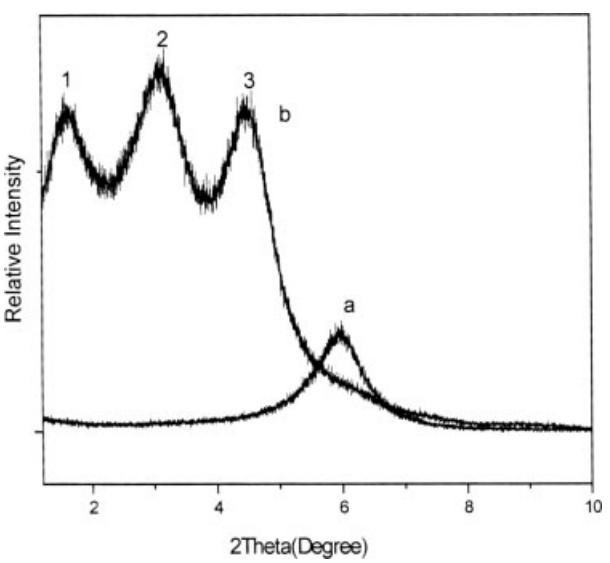

Figure 2 WAXD spectra of (a) MMT and (b) OMMT.

TABLE I
WAXD Data of MMT and OMMT

Serial no.	λ (Å)	2θ (°)	*d* (nm)
a	1.54056	6.036	1.46303
b-1	1.54056	1.680	5.25419
b-2	1.54056	3.172	2.78303
b-3	1.54056	4.540	1.94473

$2d \sin\theta = n\lambda$ corresponds to the wavelength of the X-ray radiation used in the diffraction experiment; θ, the measured half diffraction angle or glancing angle; λ to the wavelength of the X-ray radiation used in the diffraction experiment.

penetrate the layers and swell. A schematic depiction of the intercalation process between the original MMT and the intercalation agent is illustrated in Figure 3. The interlayer spacing of OMMT is so large (5.25 nm) that it is greater than the extended chain length of *N*,*N*-di(2-hydroxyethyl)-*N*-dodecyl-*N*-methyl ammonium chloride. The underlying mechanism may be related to the special structure of this intercalation agent, such as the strong polarity of the —OH groups, the branching chains of dihydroxyethyl, and the space distribution morphology of the molecular chains.

Analysis of OMMT-MB

OMMT-MB was prepared by solution intercalation, and the schematic process is shown in Figure 4. The gum of HTV-SR was first dissolved in toluene, and a homogeneous solution was obtained. The van der Waals force between silicate layers was overcome by a huge shearing force produced by a stirrer, and thus the SR molecular chains could easily be inserted into the silicate layers. The SR matrix together with nanometer silicate layers, that is, the OMMT-MB, was thus prepared. The OMMT-MB was then applied to the mixing process of HTV-SR by masterbatch techniques. The OMMT nanosilicate layers could uniformly disperse in the SR matrix, the nanoeffect of which could then be embodied.

Analysis of the HTV-SR composites

Tensile properties

As shown in Table II, the tensile properties of the HTV-SR/OMMT and HTV-SR/OMMT-MB systems were all much higher than those of pure HTV-SR. These two types of composites showed the highest values with the addition of 20% OMMT or 20% OMMT-MB. The tensile strength and elongation at break of HTV-SR/OMMT-MB-20% were improved about 1.5 and 0.9 times, respectively, in comparison with those of HTV-SR/OMMT-20%. This was probably due to the nanoeffect of the exfoliated silicate layers. Most important, the tensile strength of HTV-SR/OMMT-MB-20% was nearly equal to that of HTV-SR/aerosilica-20%, and the elongation at break even showed much improvement.

Thermal properties

Figure 5 shows TGA curves of pure HTV-SR and different types of HTV-SR composites. The characteristic thermal parameters are the initial weight loss temperature, center temperature (the temperature at which a material shows the highest thermal degradation rate), and char residue of thermal degradation. The results are summarized in Table III. In comparison with HTV-SR/OMMT-20%, the lower initial temperature of HTV-SR/OMMT-MB-20% may have resulted from the degradation of small molecular chains of the organic intercalation agents. These mo-

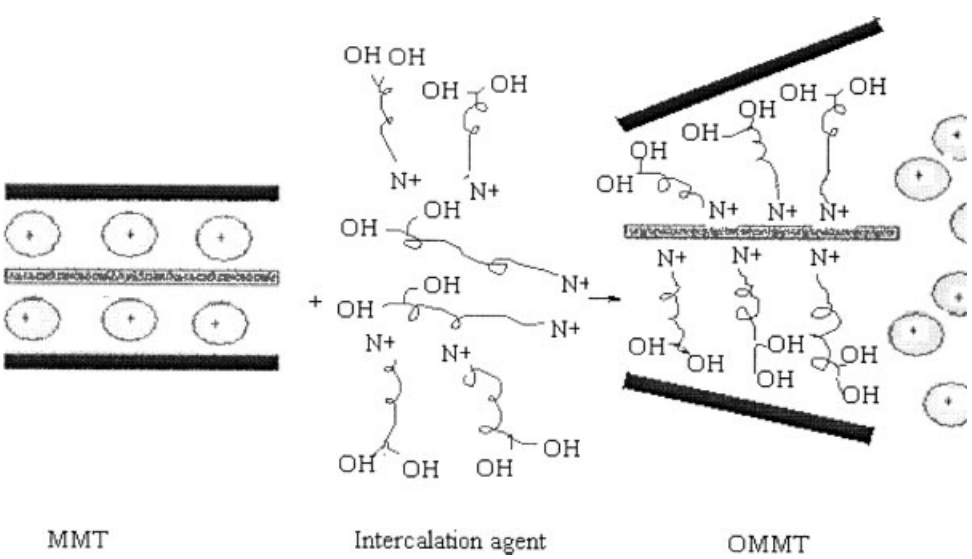

Figure 3 Scheme of the intercalation process of MMT.

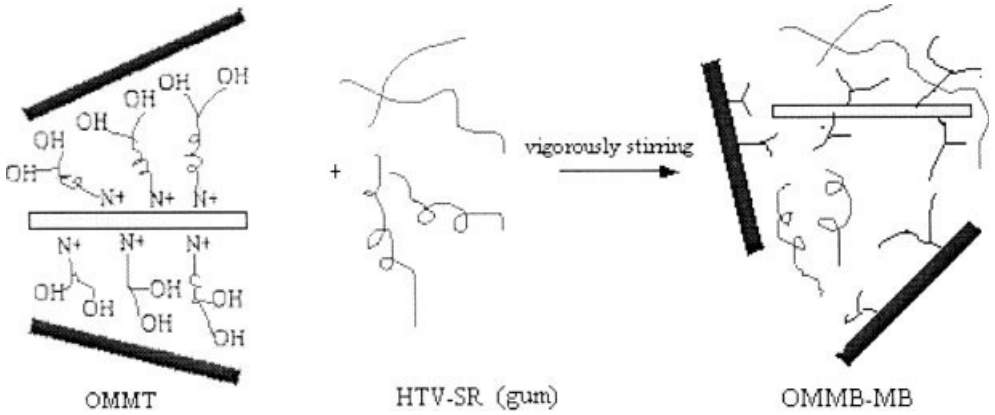

Figure 4 Scheme of the preparation process of OMMT-MB.

lecular chains covered or adhered to the nanosilicate layers of the exfoliated OMMT. The higher center temperature and amounts of char residue may be ascribed to the following two reasons. First, the exfoliated silicate layers may have retarded or impeded the heat conduction in the SR matrix; second, more thermally stable materials related to the nanosilicate layers were produced during the heating process.[21,22] In the presence of 20% aerosilica, the characteristic degradation temperatures and char residue were higher. This may have been due to the different structures and properties of the addition fillers.

Microstructure analysis

WAXD analysis

An important measure of the degree of silicate exfoliation and dispersion can be obtained by WAXD measurements. A series of WAXD patterns of composites containing 20% OMMT and OMMT-MB are shown in Figure 6. No obvious peaks can be observed in Figure 6(a), and this is due to the nature of the original microstructure of HTV-SR. When 20% OMMT-MB was incorporated, no obvious peaks were observed because of the loss of structure registry. This indicated the possibility of exfoliated silicate layers dispersed in the polymer matrix.

TABLE II
Comparison of the Tensile Properties of Different Types of HTV-SR Composites

Formulation	Filler content (wt %)	Tensile strength (MPa)	Elongation at break (%)
Pure HTV-SR	0	0.25	140
HTV-SR/OMMT	15	0.51	240
	20	0.57	260
	25	0.54	220
HTV-SR/OMMT-MB	15	0.89	390
	20	1.41	490
	25	1.21	470
HTV-SR/aerosilica	20	1.44	380

The appearance of peaks at $2\theta = 2.2^\circ$ and $2\theta = 3.5^\circ$ (d-spacing = 4.1 and 2.6 nm), which had something to do with the original OMMT [shown in Fig. 2(b)], illustrated the existence of stacked OMMT of a crystallographic order in the composites.[23–25]

TEM analysis

Further evidence of the dispersion of silicate layers in the case of HTV-SR/OMMT-MB-20% and HTV-SR/OMMT-20% composites was provided by TEM photomicrographs, as shown in Figure 7. In Figure 7(a), it can be observed that most silicate layers were dispersed homogeneously in the matrix. The dark zones are the cross sections of the silicate layers. The thickness of the silicate layers of OMMT (dark lines) was about 1 nm. The distance between most of the silicate layers was more than 10 nm, which was far larger than the original silicate layer spacing of 1.9–5.2 nm. This is evidence that these OMMTs were

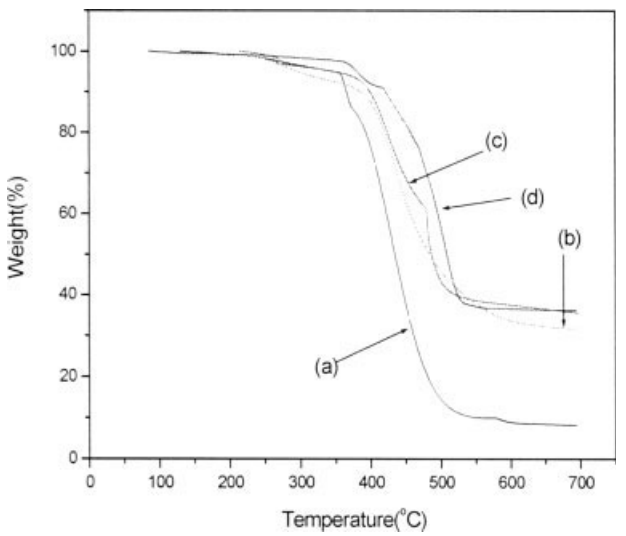

Figure 5 TGA curves of (a) pure HTV-SR, (b) HTV-SR/OMMT-20%, (c) HTV-SR/OMMT-MB-20%, and (d) HTV-SR/aerosilica-20%.

TABLE III
Comparison of TGA Data of Different Types of HTV-SR Composites

Material	Filler content (wt %)	Initial temperature of thermal degradation (°C)	Center temperature of thermal degradation (°C)	Char residue (%)
Pure HTV-SR	0	220	390	8.2
HTV-SR/OMMT	20	250	440	31.8
HTV-SR/OMMT-MB	20	230	470	35.6
HTV-SR/aerosilica	20	270	490	36.2

mostly exfoliated in the matrix. As shown in Figure 7(b), more clusters or agglomerated particles were detected, and this resulted in the lower physical properties of the system.

FTIR analysis

The microdomain structure of pure HTV-SR and different HTV-SR composites was analyzed by FTIR, as shown in Figure 8. It was found that the positions of the peaks for distinctive functional groups were almost identical in the pure HTV-SR and composites. This means that the segmented structure of HTV-SR was not affected much by the presence of OMMT and aerosilica.[26] In comparison with pure HTV-SR, detectable changes could be seen at 800, 1280, 1410, and 2800–2900 cm^{-1} in HTV-SR/OMMT-20%. These were attributed to the stretching, bending, and in-plane and out-of-plane bending vibrations of $—CH_2$ and $—CH_3$ groups present in the organic intercalation agent in OMMT. The reason for the increase in the absorption peak intensity at 1070–1090 cm^{-1} was probably the increased number of Si—O groups in OMMT. Meanwhile, the stronger peaks of HTV-SR/OMMT-MB-20% at this position may have resulted from the exfoliated nanometer silicate layers, which were uniformly dispersed in the matrix. In the case of HTV-SR/aerosilica-20%, the increased absorptions at 800 and 1280 cm^{-1} were related to the stretching and bending vibrations of Si—O groups in the aerosilica.

Mechanism analysis

Exfoliation mechanism

A rigorous thermodynamic treatment based on the lattice-based mean field theory of Vaia and Giannelis[27,28] indicates that nanostructure formation occurs if the free energy change per interlayer volume (ΔF_V) is negative. ΔF_V can be expressed as

$$\Delta F_V = \Delta E_V - T\Delta S_V \quad (1)$$

where ΔE_V and ΔS_V are the enthalpy and entropy changes per interlayer volume, respectively, and T is the temperature. Because small increases in the gallery spacing do not strongly affect the total entropy change, intercalation will rather be driven by the changes in the total enthalpy:[29]

$$\Delta E_V = \varphi_1\varphi_2\frac{1}{Q}\left(\frac{2}{h_0}\cdot(\varepsilon_{sp}-\varepsilon_{sa})+\frac{2}{r}\varepsilon_{ap}\right) \quad (2)$$

where φ_1 and φ_2 are the interlayer volume fractions of the intercalated polymer and tethered surfactant chains, respectively; Q is a constant near unity; h_0 is the initial gallery height of the organoclay; and r is the radius of the intercalation surface of tethered surfactant chains. ε_{sp}, ε_{sa}, and ε_{ap} represent the intercalation energies per area between the layered silicate and the polymer, the layered silicate and the intercalation agent, and the intercalation agent and the polymer, respectively. In terms of the HTV-SR/OMMT-MB-20% nanocomposite, the addition of OMMT-MB increased the polarity of the matrix. The interactions between the intercalation agent and the polymer and between the layered silicate and the polymer were also increased to the highest values, and this led to the most favorable ε_{ap} and ε_{sp} values. Therefore, there was a favorable excess enthalpy to enhance the dispersion of OMMT, resulting in the formation of exfoliated nanostructures. When 20% OMMT was directly incorporated, the interactions between the intercalation agent and the polymer and between the layered silicate and

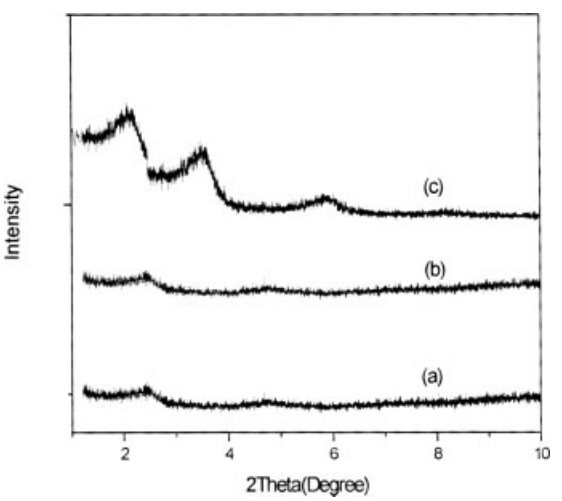

Figure 6 WAXD curves of (a) HTV-SR, (b) HTV-SR/OMMT-MB-20%, and (c) HTV-SR/OMMT-20%.

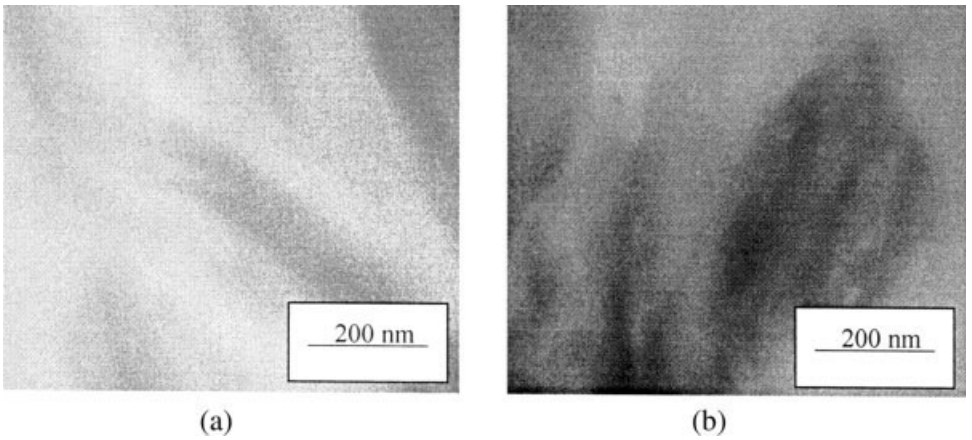

Figure 7 TEM photographs (100,000×) of (a) HTV-SR/OMMT-MB-20% and (b) HTV-SR/OMMT-20%.

the polymer were reduced, and this resulted in decreased ε_{ap} and ε_{sp} and a decrease in the enthalpy. This could decrease the dispersion degree of OMMT and make OMMT agglomerated in the matrix.

Reinforcing mechanism

The large increase in the tensile strength and elongation at break of HTV-SR/OMMT-MB-20% and HTV-SR/OMMT-20% can be attributed to the dispersion of the silicate layers in the crosslinked matrix. The different crack characteristics of the pure HTV-SR, HTV-SR/OMMT-MB-20%, and HTV-SR/OMMT-20% under tensile strength are depicted in Figure 9. The reasons for the difference can be related to parameters such as the bound elastomer (continuous elastomer matrix restricted by silicate layers), elastomer shell creation (voids in the elastomer) in the vicinity of silicate layers, and occlusion of the elastomer within the clay galleries. Thus, an increase in the tensile strength was expected when OMMT was incorporated. The failure of the three specimens upon tensile strength started with small cracks. If an elastomeric network is capable of dissipating the input energy (e.g., by conversion into heat), then it can withstand higher stresses. In the pure HTV-SR, numerous voids (subcritical cracks) appeared during drawing, and cracks were generated via voiding [shown in Fig. 9(a)]. The fracture mechanism of HTV-SR/OMMT-MB-20% was assumed to be platelet orientation, chain slippage, and zigzag energy dissipation. The nanoeffect of the silicate layers could restrict the movement of polymer chains and combine them with silicate layers. This may have reduced the number and size of voids in their vicinity [shown in Fig. 9(b)]. The increase in the crack path around the silicate layers (zigzag route) could also be considered a mechanism of energy dissipation. By this suggested model, the increase in tensile properties seems to be as expected for this clay-reinforced nanocomposite. Furthermore, in comparison with HTV-SR/OMMT-MB-20%, the decrease in the tensile strength with the direct addition of OMMT can be explained by the onset of large agglomerates. This may have decreased the crack path around the silicate layers [shown in Fig. 9(c)] and favored the initiation of catastrophic failure.[30]

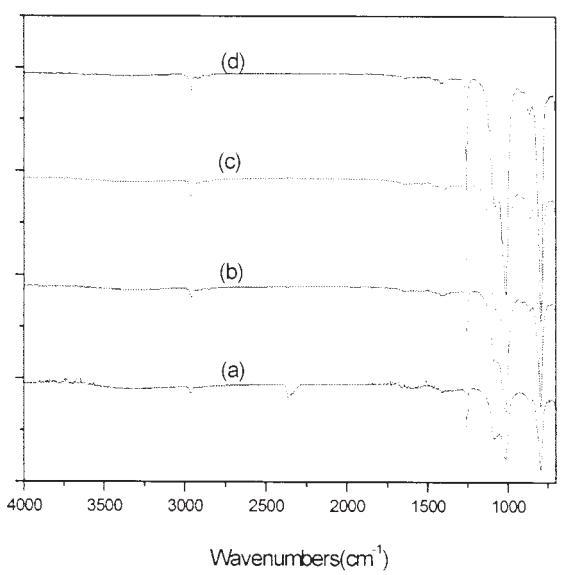

Figure 8 FTIR spectra of (a) HTV-SR, (b) HTV-SR/OMMT-20%, (c) HTV-SR/OMMT-MB-20%, and (d) HTV-SR/aerosilica-20%.

CONCLUSIONS

OMMT-MB was prepared by solution intercalation, and it was successfully applied to an HTV-SR system.

FTIR, WAXD, and TEM results verified the incorporation of this OMMT-MB into an HTV-SR matrix. They revealed that the degree of basal-spacing

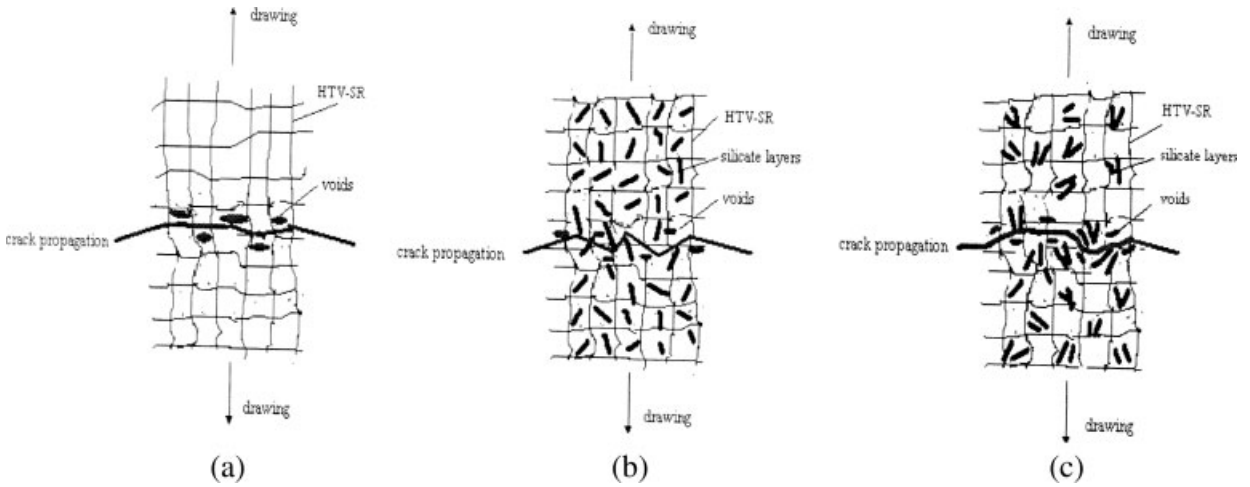

Figure 9 Scheme of failure development during tensile drawing: (a) HTV-SR, (b) HTV-SR/OMMT-MB-20%, and (c) HTV-SR/OMMT-20%.

expansion was largely increased, and an exfoliated nanostructure was formed.

The tensile strength and elongation at break of HTV-SR/OMMT-MB-20% were improved about 1.5 and 0.9 times, respectively, in comparison with those of HTV-SR/OMMT-20%. This was probably related to the nanoeffect of the exfoliated silicate layers. Moreover, the tensile strength of HTV-SR/OMMT-MB-20% was nearly equal to that of HTV-SR/aerosilica-20%, and the elongation at break even showed much improvement. In comparison with HTV-SR/OMMT-20%, the thermal degradation center temperature of the HTV-SR/OMMT-MB-20% nanocomposite was increased by 30°C. The enhanced tensile and thermal properties demonstrated the efficient reinforcing and thermal stability properties of the exfoliated and well-dispersed silicate layers in the SR matrix.

References

1. Lan, T.; Kaviratna, P. D.; Pinnavaia, T. J. Chem Mater 1995, 7, 2144.
2. Vaia, R. A.; Jandt, K. D.; Kramer, E. J. Macromolecules 1995, 28, 8080.
3. Giannelis, E. P. Adv Mater 1996, 8, 29.
4. Alexandre, M.; Dubois, P. Mater Sci Eng R 2000, 28, 1.
5. Hachett, E.; Manias, E.; Giannelis, E. P. Chem Mater 2000, 12, 2161.
6. Bujdak, J.; Hachett, E. P.; Giannelis, E. P. Chem Mater 2000, 12, 2168.
7. Fu, X.; Qutubuddion, S. Polymer 2001, 42, 807.
8. Yoon, J. T.; Jo, W. H.; Lee, M. S. Polymer 2001, 42, 329.
9. Usuki, A.; Tukigase, A.; Kato, M. Polymer 2002, 43, 2185.
10. Joly, S.; Garnaud, G.; Ollitrault, R. Chem Mater 2002, 14, 4202.
11. Zhang, W.; Chen, D.; Zhao, Q. Polymer 2003, 44, 7953.
12. Arroyo, M.; Lopez-Manchado, M. A.; Herrero, B. Polymer 2003, 44, 2447.
13. Wang, J. C.; Chen, Y. H.; Jin, Q. Q. Macromol Chem Phys 2005, 206, 2512.
14. Zhou, N. L.; Xia, X. X.; Wang, Y. R. Acta Polym Sinica 2002, 2, 253.
15. Zheng, J. P.; Li, P.; Hao, W. L. J Tianjin Univ 2000, 33, 670.
16. Alexandre, M.; Dubois, P. Mater Sci Eng 2000, 28, 1.
17. Han, B. H.; Cheng, A. M.; Ji, G. D. J Appl Polym Sci 2004, 91, 2537.
18. Ma, J.; Xu, J.; Ren, J. H. Polymer 2003, 44, 4619.
19. Wei, F.; Abdellatif, A. K.; Bernard, R. Macromol Rapid Commun 2002, 23, 705.
20. Chen, T. K.; Tien, Y. I.; Wei, K. H. Polymer 2000, 41, 1347.
21. Yano, K.; Usuki, A.; Okada, A. J Polym Sci Part A: Polym Chem 1993, 31, 2493.
22. Shengpei, S.; David, D. J.; Charles, A. W. Polym Degrad Stab 2004, 84, 274.
23. Xu, R. J.; Manias, E.; Alan, J. S.; Runt, J. Macromolecules 2001, 34, 338.
24. Yao, K. J.; Song, M.; Hourston, D. J. Polymer 2002, 43, 1018.
25. Konstantinos, G. G.; Nikolaos, S. S.; Anton, A. A. Macromol Mater Eng 2004, 289, 1081.
26. Rodlert, M.; Christopher, G. P.; Garamszegi, L. Polymer 2004, 45, 952.
27. Vaia, R. A.; Giannelis, E. P. Macromolecules 1997, 30, 7990.
28. Vaia, R. A.; Giannelis, E. P. Macromolecules 1997, 30, 8000.
29. Manias, E.; Touny, L.; Wu, K.; Strawhecher, B. Chem Mater 2001, 13, 3516.
30. Mousa, A.; Karger-Kocsis, J. Macromol Mater Eng 2001, 286, 260.